Journal of
Manufacturing and Materials Processing

MDPI

Article

Ring Beam Modulation-Assisted Laser Welding on Dissimilar Materials for Automotive Battery

Se-Hoon Choi [1], Jong-Hyun Kim [2] and Hae-Woon Choi [2,*]

[1] Graduate School of Mechanical Engineering, Keimyung University, Daegu 42601, Republic of Korea; csh813@naver.com
[2] Department of Mechanical Engineering, Keimyung University, Daegu 42601, Republic of Korea; kimjh@kmu.ac.kr
* Correspondence: hwchoi@kmu.ac.kr; Tel.: +82-53-580-5215

Abstract: This paper investigates Ring Beam Modulation-assisted Laser (RBML) welding as a novel approach for joining dissimilar materials, specifically aluminum and copper, which are essential in high-performance applications such as electric vehicle batteries and aerospace components. The study aims to address challenges such as thermal mismatches, brittle intermetallic compounds, and structural defects that hinder traditional welding methods. The research combines experimental and computational analyses to evaluate the impact of heat input distributions and laser modulation parameters on weld quality and strength. Three welding cases are compared: fixed center beam with variable ring beam outputs, variable center beam with fixed ring outputs, and a wobble-mode beam to enhance interfacial bonding. Computational modeling supports the optimization process by simulating heat flows and material responses, exploring various shape factors, and guiding parameter selection. Key findings include a nonlinear relationship between heat input and welding strength across the cases. Case 1 demonstrates improved weld strength with higher ring beam input, while Case 2 achieves excellent reliability with relatively lower inputs. Case 3 introduces wobble welding, yielding superior resolution and consistent weld quality. These results confirm that precise ring beam modulation enhances weld reliability, minimizes thermal distortions, and optimizes energy consumption. The manuscript advances the state of knowledge in laser welding technology by demonstrating a scalable, energy-efficient method for joining dissimilar materials. This contribution supports the fabrication of lightweight, high-reliability assemblies, paving the way for innovative applications in the automotive, medical, aerospace, and shipbuilding industries.

Keywords: laser welding; beam modulation; dissimilar material; aluminum and copper; EV battery

Academic Editors: Daniel F.O. Braga and Sérgio Tavares

Received: 23 December 2024
Revised: 15 January 2025
Accepted: 20 January 2025
Published: 21 January 2025

Citation: Choi, S.-H.; Kim, J.-H.; Choi, H.-W. Ring Beam Modulation-Assisted Laser Welding on Dissimilar Materials for Automotive Battery. *J. Manuf. Mater. Process.* **2025**, *9*, 28. https://doi.org/10.3390/jmmp9020028

1. Introduction

Eco-friendly innovations such as electric mobility are encountering obstacles including the depletion of resources and global warming [1]. The battery is the pivotal component that plays the most critical role in the transition from internal combustion engine vehicles to future vehicles. Not only are lightweight packages required to improve mobility efficiency, but high-strength materials and designs that can protect components from external impacts are required. Through research and development, traditional combustion engine-powered vehicles have provided durable and high standards to users. Therefore, the components that serve as the key to future vehicles must be sufficiently stable and protected from shock and corrosion [1–3].

Automobiles have been constructed with complex structures and various metal materials to enhance reliability. Increasing steel strength in components and modules is a common practice, but this entails unnecessary structure and weight. To reduce weight and improve driving efficiency, the thickness of steel can be reduced. However, the strength is also reduced, and the manufacturer's investment in optimization design and verification increases. Recently, methods have emerged to assemble various materials and appropriately utilize their individual characteristics effectively. For example, batteries connect multiple materials to achieve efficient packaging and performance [1,4–10].

Mainly, batteries consist of hundreds to thousands of cells connected in series, each very sensitive to assembly. However, materials exhibiting high electrical and thermal conductivities, such as copper and aluminum, are generally termed "difficult to weld" [1,6,8]. Mechanical assembly using bolts, etc., is traditionally available, but problems such as structural deformation may occur because high pressure is applied. Using chemical adhesives can reduce weight with a simple process, but adhesives have the weakness of losing strength due to temperature or humidity. To overcome these limitations, welding techniques have been developed for the copper cathodes and the aluminum anodes; ultrasonic, resistance-spot, and laser welding are employed to this end [1–3]. Ultrasonic welding is a solid-state method that converts high-frequency electrical energy into mechanical vibration to generate heat between the bonding interfaces. Since ultrasonic welding is a reliable process, it is used principally to form tap-tap and tap-bus bar joints. However, the equipment is ordinarily expensive and challenging to operate in confined spaces [1,4–7]. Arc or electric resistance welding is common and has a favorable technical approach for users, but it is not easy to achieve high-quality welding of dissimilar materials. The joint will fail because of its low precision controllability if the heat input is insufficient. At the other extreme, intermetallic compounds will form at the joint interface if excessive heat is applied, causing damage and reducing the weld's strength and durability [9].

Laser welding is a facile method that enables automated production and is thus commonly used to manufacture components [11–14]. Compared to the other joining techniques described above, the area to be processed by heat can be minimized. Therefore, the mechanical and electrical properties of the material are adequately protected, because external forces and chemical impacts are not entailed [11,15,16]. Laser welding of dissimilar materials uses low photon energy to preserve material properties, so the reduction of laser absorption due to optical reflection on the material surface is a crucial factor in reducing the quality of the joint. Methods to modulate the laser power more precisely, in a pattern, or to use multiple beams have also been studied. Moreover, laser keyhole welding of dissimilar materials, specifically for battery welding applications, offers outstanding advantages [16–18].

The focused laser beam can create a deep, narrow, keyhole-shaped penetration into the materials, allowing fast and efficient welding with minimal heat input. Laser keyhole welding can achieve high welding speeds, significantly increasing the productivity and efficiency of battery welding processes. The small heat-affected zone and minimal thermal distortion associated with laser keyhole welding allow for precise control over the welding process, resulting in high-quality and consistent welds [15,16]. Since accurate and reliable assembly processes are essential to ensure battery integrity and performance, keyhole laser welding machining advantages can be well-utilized in battery component assembly. The keyhole laser can penetrate the battery materials, enabling the reliable welding of thick and multi-layered battery components. The ability to create deep and narrow welds with a single pass reduces the need for multiple welding passes, saving time and improving efficiency in battery welding. Energy efficiency is significant compared to traditional welding methods. The focused laser beam delivers energy precisely to the desired welding

area, minimizing heat loss to the surrounding materials [13]. This results in reduced energy consumption and lower operating costs. These advantages make laser keyhole welding a preferred choice for battery welding applications, improving productivity, quality, and cost-effectiveness in producing batteries for various industries, including electric vehicles, consumer electronics, renewable energy storage, and more [11–15].

Dual-beam laser welding is advancing manufacturing sectors, including automotive, aerospace, and EV battery production. It enables the precise joining of dissimilar materials, such as aluminum and copper, which are challenging due to their differing physical and chemical properties [19–22]. Issues such as intermetallic compound (IMC) formation, heat input control, and thermal mismatches hinder traditional welding. Dual-beam systems improve energy distribution and joint quality [19,21]. Combining core and ring laser beams, dual-beam systems control energy input for pre-heating, welding, and post-heating. This minimizes IMC formation and enhances tensile strength [10,22].

Tools like CFD and meta-models optimize process parameters for joint geometry, heat distribution, and defect mitigation. Empirical studies validate simulations, refining welding parameters to ensure quality and scalability [10,20,22]. Dual-beam welding reduces defects like cracks and porosities, improving manufacturing throughput and product reliability. These techniques enable the scalable production of lightweight, high-performance assemblies for diverse applications, from EV batteries to aerospace. Developing real-time monitoring systems and extending methodologies to more material combinations can increase adoption and industrial impact [10,19–22].

To study dissimilar material welding, it is important to understand the material interaction between lasers and materials. Molecular dynamics simulations and experimental verifications have been carried out to address challenges in integrating graphene with Cu nanoparticles for advanced interconnect materials. These studies determined that graphene slows the sintering process while enhancing mechanical properties such as shear strength and reducing porosity. Simulating various sintering temperatures, it demonstrated that higher temperatures accelerate sintering, improving its efficiency, thus validating the applicability of graphene-Cu composites in high-performance, low-temperature scenarios [23,24].

To understand a laser's material interactions with dielectric materials, laser ablation of alumina-zirconia composites was carried out to investigate the potential for medical implants, highlighting how varying alumina content influences material removal rates, thermal cracking susceptibility, and laser ablation thresholds. Composite materials showed lower ablation thresholds compared to single-phase materials, suggesting their higher machinability. Insights from this study offer significant implications for optimizing laser parameters and material compositions to improve the performance of dental and orthopedic implants [25,26]. Femtosecond laser fabrication of infrared micro-optical devices focus on leveraging advanced laser processing for hard and brittle materials. By combining etching and laser techniques, it enables precise three-dimensional structuring of infrared optical components, including microlenses and anti-reflective structures. These advancements demonstrate significant applications in fields like aerospace, biomedical imaging, and infrared detection systems [24–26].

Laser modulation is another way to improve weld quality. High-density laser welding creates a rapid temperature rise in the material, and the rapid decrease makes the weld brittle. Studies have improved welding quality via real-time pre-heating, welding, or post-heating [6,10]. However, the increase in processing time increases the cost and reduces productivity [10,16]. To encounter the problem, real-time modulation methods such as dual-beam and transverse mode are used [17,18,27,28]. Laser beam modulation refers to the intentional variation of the characteristics of a laser beam, such as its intensity, frequency, or

phase, over time [10,27,28]. Thus, we suggest that the laser with modulation is appropriate to increase the absorption of difficult to weld materials such as copper and aluminum. Still, the effect of laser beam modulation can vary depending on the specific modulation technique and its parameters. Keyhole laser welding with modulation is quick and energy-dense. Studying the complex energy behavior within the weld pool is a challenge. Ultrafast lasers can be used to weld transparent materials, leveraging nonlinear absorption and precise energy deposition to achieve localized thermal effects and melt pool control [29]. It can minimize the accumulation of heat through high-repetition-rate lasers, dynamic plasma morphology management, and spatial/temporal shaping, which enhance melt pool flow stability and enable advanced applications in transparent and heterogeneous material joining [29].

This research introduces Ring Beam Modulation-assisted Laser (RBML) welding as a novel technique for joining dissimilar materials like aluminum and copper, addressing challenges such as thermal mismatches and brittle intermetallic compounds. The findings demonstrate enhanced weld quality, energy efficiency, and reliability through optimized laser modulation, with applications in industries like electric vehicles and aerospace. However, the study is limited to specific materials and parameters. Future research should explore a wider range of materials, adaptive laser modulation, and long-term joint performance under operational conditions to expand the technique's industrial applicability.

Here, we propose state of the art beam modulation of the laser into the core and ring. The specimens are fabricated using a multi-beam laser. The welding characteristics of copper and aluminum under various heat input distributions were studied theoretically and experimentally. The optimal heat input and methodology were obtained by analyzing the weld cross-section and tensile load. We performed computer simulations to ensure the reliability of the laser machining technology. In addition, the computational analysis developed an optimal balance of core and ring laser power, which may reduce the significant thermal mismatch in laser welding. We expect that the proposed compelling idea of assembling dissimilar materials will contribute to the processing of lightweight and multi-property components and assemblies. Furthermore, the idea can be extended to apply to various industries such as batteries, aerospace, and medical devices.

2. Methodology

2.1. Combining Two Lasers

The dual-beam laser welding technique introduces a novel approach by integrating a core and ring laser beam to optimize the welding process. This configuration enables precise control over the pre-heating, welding, and post-heating phases, addressing critical challenges like thermal mismatches and defect formation in dissimilar material joints. In addition, the ring beam modulation-assisted laser can optimize heat distribution and energy efficiency, overcoming challenges in joining dissimilar materials like aluminum and copper for high-performance applications in industries such as automotive and aerospace.

As shown in the conceptual principle in Figure 1a, the proposed Ring Beam Modulation-assisted Laser (RBML) welding operates simultaneously with a core laser and a ring laser. The laser system (FL8000-ARM, Coherent Inc., Saxonburg, PA, USA) used in the experiment was a multi-mode fiber laser with Max. power of 8 kW. The wavelength was 1070 $\pm$ 10 nm and the beam quality (BPP) at the collimator were less than 4 mm·mrad and $\leq$14 mm·mrad for the center beam and ring beam, respectively. The type of fiber optic cable interface was QBH (Quartz Block Head), and the fiber core diameters were 70 µm and 180 µm for the center and ring, respectively. The measured laser beam diameter was 800 µm, and same diameters of laser beam were used for all cases.

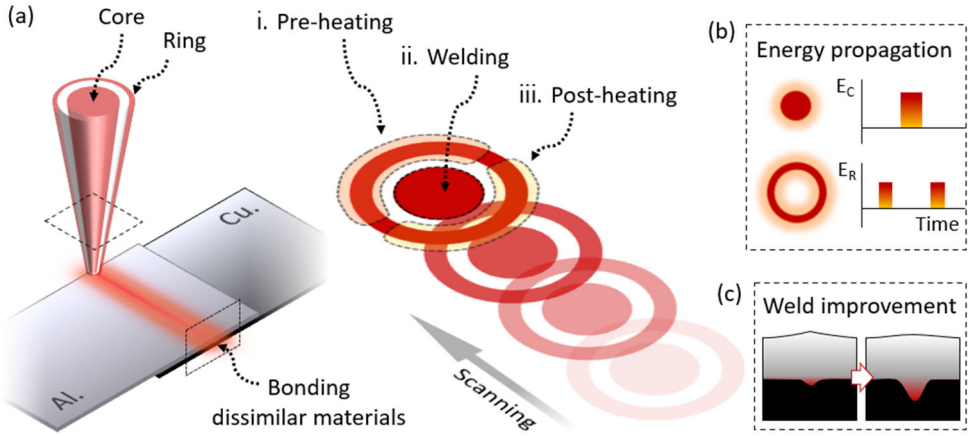

Figure 1. Principle of the idea (**a**) dual-beam laser welding for dissimilar materials (**b**) Energy propagation of the Ring Beam Modulation-assisted Laser Welding (**c**) Weld reliability improvement through ring laser.

The flexibility of beam shaping has been utilized to provide versatility and adaptability in a wide range of laser applications. In the proposed study setup, the beam generated is transmitted through an optical fiber to a laser scanner and then irradiated onto the specimen. The core and ring lasers can be efficiently coupled to an optical fiber, delivering the laser beam to a remote processing location [10,12,17]. The core and ring lasers can form an effective area by focusing. Focused to a spot size, the lasers can provide high resolution and fine local welding [10,12]. The dual lasers can provide various output power combinations. RBML is easy to configure and has excellent beam quality due to its symmetrical beam profile. RBML could be advantageous in fields requiring precise and delicate bonding technology, such as secondary battery manufacturing, which requires assembling heterogeneous materials. Therefore, we studied the optimization of laser welding that supports the modulation of RBML and analyzed the bonding quality of RBML-based aluminum and copper. As a result, our experimental analysis contributes to the development of sophisticated laser welding techniques.

2.2. Ring and Core Modulation

Laser scanning shows that the front of the preceding ring beam (area i) provides pre-heating. Then, the central core beam (area ii) that follows the ring can perform keyhole or conduction welding. Finally, the rear of the entailed ring beam (area iii) performs post-heat treatment to control the cooling rate of the welding zone. The joining materials used in the experiment were 6000 series aluminum alloy made of Al-Mg-Si as the primary alloying element.

In general, cracks can occur due to heat input in the welding process and must be controlled. In particular, when welding aluminum, cracks can occur if hydrogen is not released due to the difference in hydrogen solubility during melting and solidification, which forms pores and defects in the welding zone of the joining interface. As the counterpart of aluminum alloy for bonding, we employed oxygen-free copper, a material that is melted and cast in a hydrogen stream or a vacuum. This material's electrical and thermal conductivities are plentiful, but hydrogen is sparse. Yet, absorption of a near-infrared laser beam (wavelength 1 μm) is insufficient; thus, the welding is unfavorable. Therefore, surface pre-heating or quick quenching is advantageous for bonding. RBML, which provides both pre-heating and post-heating, is an appropriate solution.

As shown in Figure 1b, the core and the ring can control energy propagation using the proposed dual beam. The laser scanning speed dominates the frequency of the energy ex-

posure. The number of energy propagations is constrained by the simultaneously exposed core and ring lasers. The frequency of the core and the ring can be adjusted according to the diameters of the core and the ring. Above all, if the energy magnitudes of the core and the ring can be facilely controlled and the interrelationship according to the energy ratio of the core and the ring is analyzed, the RBML optimization can be achieved most efficiently. The energy balance equation for the energy-based machining can be described as Equation (1):

$$\int_V \rho U dV = \int_S q dS + \int_V r dV \quad (1)$$

where U is the rate of internal energy, q is the specific heat flux [W/(kg·m^2)], and r is the work of the external system [J]. Quenched energy travels via convection and conduction through the interiors of the two metals. The conductive transfer is given by the Fourier Equation (2):

$$\int_V \rho U \delta\theta dV + \int_V \frac{\partial \delta\theta}{\partial x} k \frac{\partial \theta}{\partial x} dV = \int_V \delta\theta r dV + \int_S \delta\theta q dS \quad (2)$$

where θ is the temperature [K] and k is the coefficient of thermal conductivity [W/(m·K)]. The coordinate system must consider time during laser welding since the heat source moves with time. Heat conduction during welding is associated with significant temperature changes and thus material thermal conductivities and specific heats. The three-dimensional heat transfer equation when the heat source moves over time is Equation (3):

$$\frac{\partial}{\partial x}\left(k\frac{\partial T}{\partial x}\right) + \frac{\partial}{\partial y}\left(k\frac{\partial T}{\partial y}\right) + \frac{\partial}{\partial z}\left(k\frac{\partial T}{\partial z}\right) + q = \rho c \quad (3)$$

where ρ is the density [kg/m^3] and c is the specific heat [J/(kg·K)]. As shown in Figure 1c, the quality of RBML can be improved through theoretical and experimental studies of RBML. Laser energy penetration produces robust welds. Through the RBML, the energy consumption in machining will be effectively controlled, and reliable welding will appear over a minimal area.

2.3. Computational Modeling

A computer simulation utilizing the optics module of COMSOL (version 5.2) was employed to examine heat flow during dissimilar material joining. In this study, we introduce the simulation model that correlates the temperature distribution within the weld zone to assess heat flow. A detailed computational approach, including longitudinal heat distribution (depicted by the comet-tail profile), along with validation and microscopic analysis, was presented in our prior research [10,12,16,22]. The weld pool is primarily influenced by convective heat flow. However, due to the thin profile of the weld pool and the high welding speed, conduction heat distribution can be reasonably assumed for accurately estimating the weld joint geometry. The boundary condition is forced air convection. Since boundary conditions are essential in defining the behavior of heat flow in the material, forced air convection conditions are referred to in our previous experimental data [16]. The symmetry boundary condition representing a symmetry plane's presence in the computational domain is used. The airflow is symmetric, and no flow or heat transfer occurs across the symmetry plane. This boundary condition allows for a reduction in computational requirements and simulation time. A Gaussian beam is set to simulate the core beam profile. The Rectangle function is based on the internal function, and the Delta function is modified and applied to the ring mode or outer beam profile. To model this situation, we suppose that the outer laser is uniformly distributed over the upper and lower boundaries, which are the outer diameter and inner diameter, respectively [16]. We explore

temperature distributions and cooling rates based on the heat inputs and beam shapes, as well as derived thermal expansion and contraction with temperature. The inputs are the heat parameters, the welding speeds, the boundary conditions, and the material properties. The power is assumed as a Gaussian distribution as described in Equation (4):

$$Q(x,y,z) = Q_0(1-R_c)\frac{A_c}{\pi\sigma_x\sigma_y P_{dp}} e^{-[\frac{(x-x_0)^2}{\sigma_x^2}+\frac{(y-y_0)^2}{\sigma_y^2}]/s_f} e^{-[A_c z]} \quad (4)$$

where Q_0 is the input power, R_c is the reflectivity, sf is the shape factor,σ_x and σ_y are the beam waist x and y coordinates, and Pdp is the skin depth. The shape factor (sf) is that of the laser beam, which determines the Gaussian shape of heat input. The skin depth—the surface beam penetration depth—varies with a material's optical properties. Both simulations and real-world tests inevitably include errors, which can be minimized by repeatedly changing the shape factor and skin depth. The skin depth can be calculated in Equation (5). As the laser beam irradiates the metal, a thin layer of the surface can absorb the laser energy. If the conductivity is high, then the absorption coefficient can be calculated as shown in Equation (5). The penetration depth or skin depth for the aluminum can be calculated as $1/\alpha$. Most common conductors have a relative permeability of very near 1, so for copper, aluminum, etc., a μ value of $4\pi \times 10^{-7}$ H/m can safely be assumed.

$$\alpha = \frac{2\omega k}{c_0} \approx \sqrt{\frac{2\sigma_0\omega}{\varepsilon_0 c_0^2}} \quad (5)$$

where ω is the angular frequency, k is the wave number, and c0 is the speed of light.

2.4. Experimental Setup

The experimental setup for laser welding is shown in Figure 2a. The system features a robotic arm that stably transports the laser head for use, a laser beam delivery system that precisely transports or scans beams, and a clamping jig that fixes parts during welding.

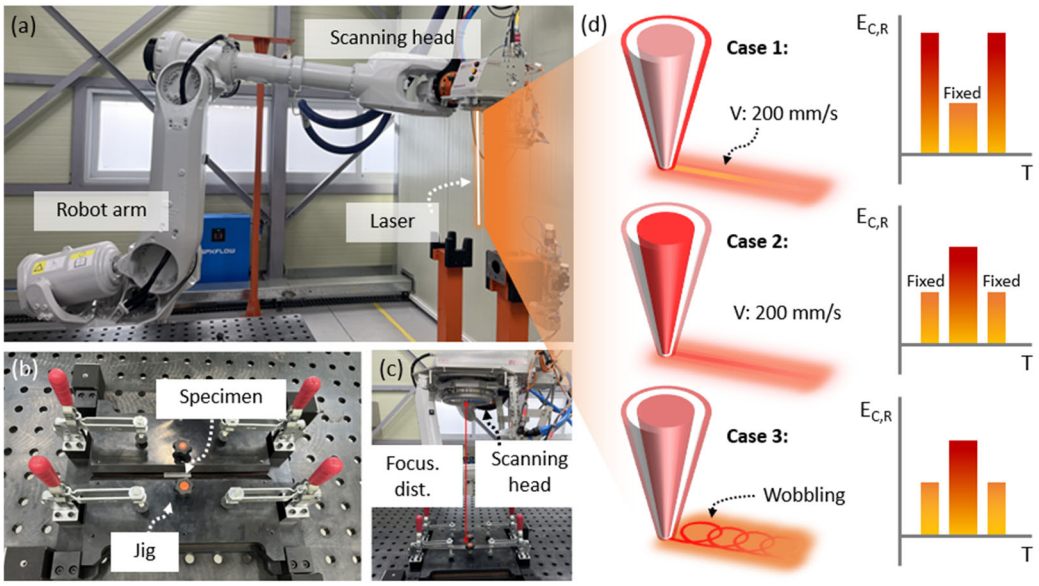

Figure 2. Experimental setup (**a**) Robot arm-based laser welding (**b**) Jig for placing target specimen (**c**) Scanning head aligned to the target (**d**) Laser variation.

The beam used by the scanner is transmitted to the scanner by the robot. Laser beam scanners are devices used in laser systems designed to control a laser beam's movement and direction. The functions of laser beam scanners are beam steering and positioning.

Laser beam scanners can accurately steer and position the laser beam at specific locations or paths. The scanning head allows for precise control of the laser beam's position and direction, enabling high-precision laser processing operations. Since the heat distribution can be customized, it is advantageous in applications that require the ability to create complex patterns or shapes, or in the welding that is part of battery assembly.

In Figure 2b, the copper is placed in the bottom jig and the aluminum in the top jig for the purpose of bonding the aluminum and copper. The dimensions of the weld specimen are tailored to a width of 50 mm, a length of 100 mm, and a thickness of 0.4 mm. To prevent the back reflection of a fiber laser from the copper surface, optical elements such as isolators or circulators are installed to allow light to pass through in one direction while attenuating or blocking light in the opposite direction.

In addition, a proper alignment and focusing of the laser beam can minimize back reflections by tilting the head from the optical axis. Thus, to prevent damage caused by high-level beam reflectance from the specimen surfaces, the entire laser beam irradiation system is tilted at about 3.8°. The delivered laser beam is transmitted to the laser beam scanning head, as shown in Figure 1c. The laser power was estimated and chosen based on findings from our prior research on welding similar materials [10]. Subsequently, the laser power and balance were adjusted in accordance with the wobbling and scanning parameters used in the welding process [10].

The transmitted optical fiber bundle comprises a core diameter of 70 μm and a ring diameter of 180 μm. The maximum transmitted power is 7.5 kW for the center fiber and 10 kW for the ring laser. This experiment used the same laser media and wavelength for a stable energy supply and welding quality comparisons. Two separate lasers can emit beams of different power or characteristics. These laser sources can be various types of lasers, such as fiber lasers, diode lasers, or solid-state lasers, and may operate in different modes, such as continuous wave or pulsed operation. As shown in Figure 2d, the experimental conditions were scheduled as Case 1: line mode (center beam fixed, ring beam variable), Case 2: line mode (center beam variable, ring beam fixed), and Case 3: wobble mode.

3. Results and Discussion

3.1. Fabrication

In Case 1, the center beam output was fixed at 800 W, the ring beam output was 1600 W to 2400 W, and the welding speed was 200 mm/s. In Case 2, the center beam output varied in 50 W steps from 950 to 1150 W, the ring beam output was fixed at 500 W, and the welding speed was set at 200 mm/s. These optimal parameters are identified via initial experiments, and the optimized procedures are performed at least five times.

3.2. Vision Analysis

To investigate the effects of pre- and post-heating through the ring beam modulation-assisted laser welding, we performed a visual analysis to figure out the cross-section of each sample. For the cross-sectional analysis, we used the Keller etch solution (H_2O 950 mL + HNO_3 25 mL + HCl 15 mL + HF 10 mL). Specimens were cut, mounted, polished, and etched, and regions with welding defects such as cracks and pores were identified.

As shown in Figure 3a, the cross-sections revealed uniform interfacial bonding throughout the welds and local finger-like welds; the copper and aluminum layers were well-mixed. Generally, the stronger the bonding strength, the more the two layers are mixed and welded. Since the laser is irradiated from top to bottom, as shown in the picture, the stronger the laser input energy, the more the structure that invades downward at the interface of the two materials develops.

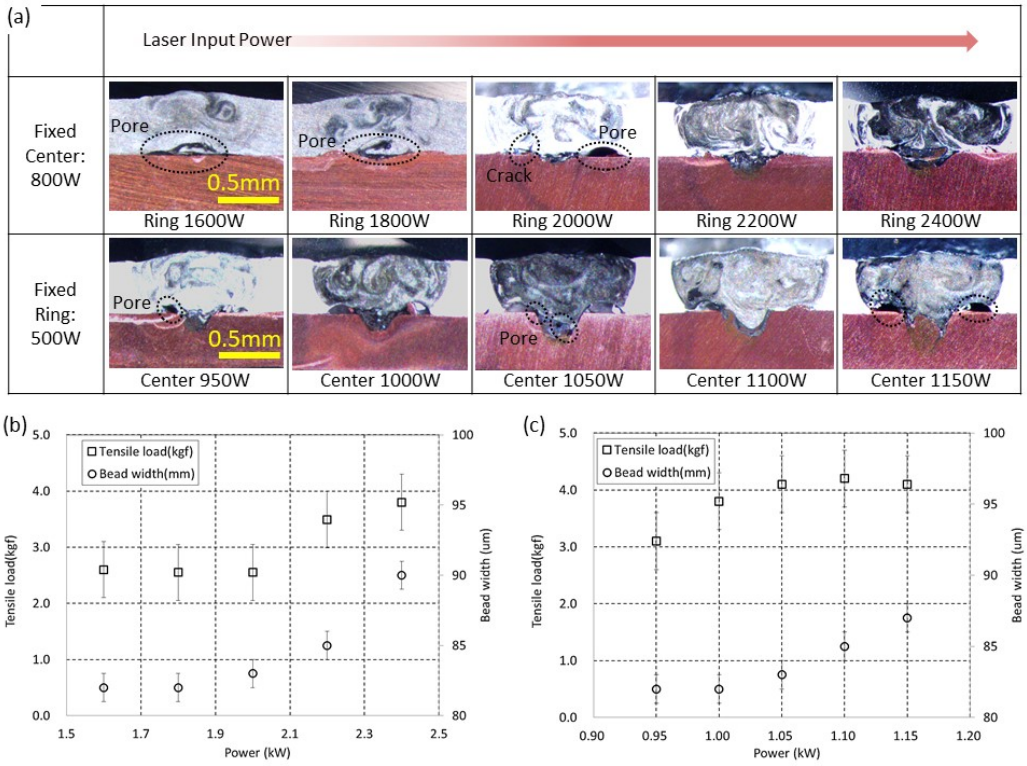

Figure 3. (**a**) Cross-sections of ring beam modulation-assisted laser welding (**b**) Tensile load and bead width vs. heat input for Case 1 (**c**) Tensile load and bead width vs. heat input for Case 2.

The shaded area in the picture mainly indicates pores. Pores occur when there is not enough support energy for bonding. In our tests, pores occurred when ring modulations of 1600 W to 2000 W and core modulations of 950 W and 1050 W were used. Pores also occur when the input energy of the ring is insufficient compared to the core; in our tests, this occurred at a core modulation of 1150 W. In addition, cracks may occur during the curing process if the post-heating is inappropriate. In our case, this occurred when the ring input power modulation was 2000 W.

3.3. Mechanical Analysis

Next, we performed a tensile test. The maximum tensile force was measured by output and condition using a lab scale tester (Cometech QC-528K4). The speed of the tensile test was 20 mm/min, and the force was evenly distributed along the 20 mm weld length. In Figure 3b, the maximum loads were 2.6 and 3.8 kgf at the minimum and maximum ring beam outputs (1.6 and 2.4 kW, respectively).

Slight deformations with no distortion were apparent in the welds and the heat-affected zones. When the center beam was fixed and the ring beam was modulated from 2200 W, not only did the tensile load increase rapidly, but also defects such as pores or cracks did not occur. This result suggests that proper support of the ring laser can effectively improve the strength and quality of laser welding. According to the significant finger-like welds in cross-sectional views, central beam modulation can provide improved welding.

In Figure 3c, the beads in the welds are quite uniform; the bead width of the upper layer is 80~90 μm depending on the output. The maximum allowable load was 3.1 kgf at 0.95 kW (the minimum center beam output) and the maximum load was 4.2 kgf at an output of 1.1 kW. The maximum allowable load decreased slightly at 1.15 kW, but the difference was within the range of error. No weld distortion or deformation was observed. The welds of Case 2 were slightly better than those of Case 1. Comparing the weld quality according to the bead width of Case 1 and Case 2, Case 2 provided a strong weld. When

the bead width of Case 1 was about 81 to 83 um, the tensile load was 2 to 3 kgf/mm, while for Case 2 it was 2.6 to 3.6 kgf/mm. When the bead width of Case 2 was about 84 to 86 um, the tensile load was 3 to 4 kgf/mm, while for Case 2 it was 3.8 to 4.8 kgf/mm.

3.4. Application: Wobble Welding

Cases 1 and 2 focused on evaluating the effectiveness of weld joint strength by varying the laser power. In contrast, Case 3 explores an alternative approach to achieving controlled heat distribution. While heat distribution can typically be managed through laser beam shaping or adjustments in laser power, we employed laser beam wobbling in Case 3 to achieve a similar effect. This technique introduces oscillatory motion to the laser beam, enabling precise control of heat distribution and potentially enhancing weld quality.

A scanning modulation, called wobbling, increases weld reliability because interfacial fusion proceeds throughout the welds, resulting in fewer pores and cracks than in non-wobble welds, as shown in Figure 3a. Here, to overcome these limitations, we adopted wobble welding. To investigate the advance of wobbling modulation, the output of the center beam was fixed at 1.1 kW and that of the ring beam at 0.6 kW (Case 3).

Wobbling was performed by varying the amplitude (rotating radius) of the laser beam from 0.1 to 0.5 mm. The wobbling frequency was 500 Hz and the linear feed rate was 200 mm/s. No shielding gas was supplied. The results are shown in the Figure 4a. The welded beads are uniform and the upper bead width range is 53~82 μm, depending on the amplitude. As the wobble amplitude increased, the maximum allowable tensile force also increased. This amplitude is linked to the wobbling frequency and welding speed. The cross-sectional view shows the uniform interfacial bonding throughout the welds; there are no pores or cracks. Figure 4b shows the tensile/shear tests. The minimum allowable load was 1.9 kgf at an amplitude of 0.5 mm, and the maximum allowable load was 3.3 kgf at an amplitude of 0.3 mm.

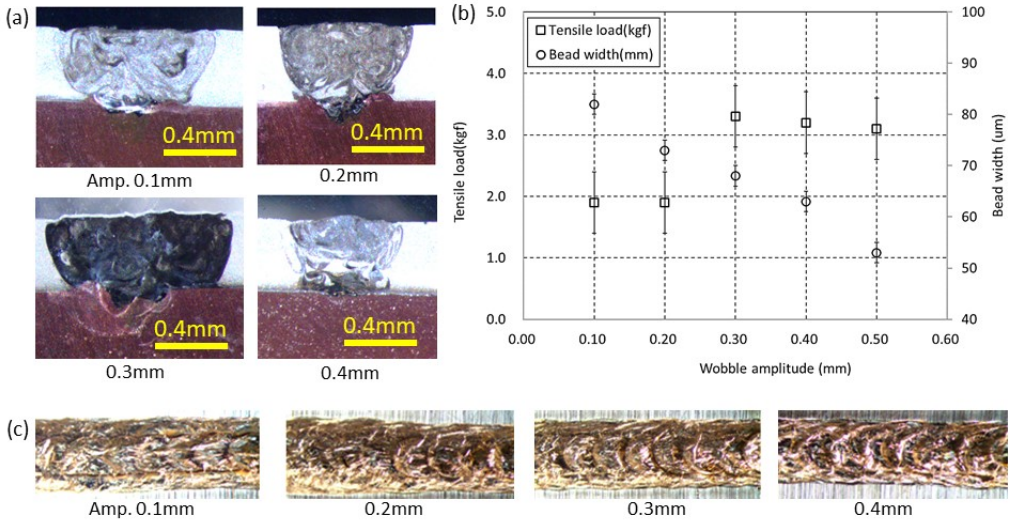

Figure 4. (**a**) Cross-sections of wobble welding (**b**) Unit tensile load (kgf/mm) and bead width vs. wobble amplitude for case 3 (**c**) Welding surfaces with various wobbling amplitudes.

Comparing Cases 2 and 3, Case 3 shows a higher resolution welding capability and improved welding quality. In Case 2, the bead width is 81~83 um when the tensile load was 2.6~3.6. In Case 3, the bead width is about 51~55 um. There are no pores or cracks. The difference is outside the error range; the maximum allowable load decreased as the amplitude increased. In the case of Figure 4c, it can be seen that the higher the overlap rate of the welding beads as the amplitude value decreases under the same welding conditions and frequency, the higher the tendency of the width of the formed welding beads to

increase. For this reason, it is judged that the bead width changes according to the value of the amplitude, affecting the maximum allowable tensile force.

3.5. Computer Simulation

Computational analyses were conducted for shape factors 1, 2, and 3. Figure 5a compares the experimental cross-sections and the simulated temperature distributions, in which the maximum temperature reached 1085 °C at the fusion boundary between dissimilar materials (dotted lines). Simulation elucidated the flow and heat distributions within dissimilar materials welded at high speeds. The shape factor and the surface penetration depth connected the simulations to real-world welding. The optimal shape factor was derived by comparing the temperature during welding measured by a thermocouple with the simulated temperature. The simulated cooling rates facilitate an understanding of the intermetallic compound layer. For shape factors between 1 and 3, the respective maximum temperatures were changed to 976.7, 857.4, and about 775 °C.

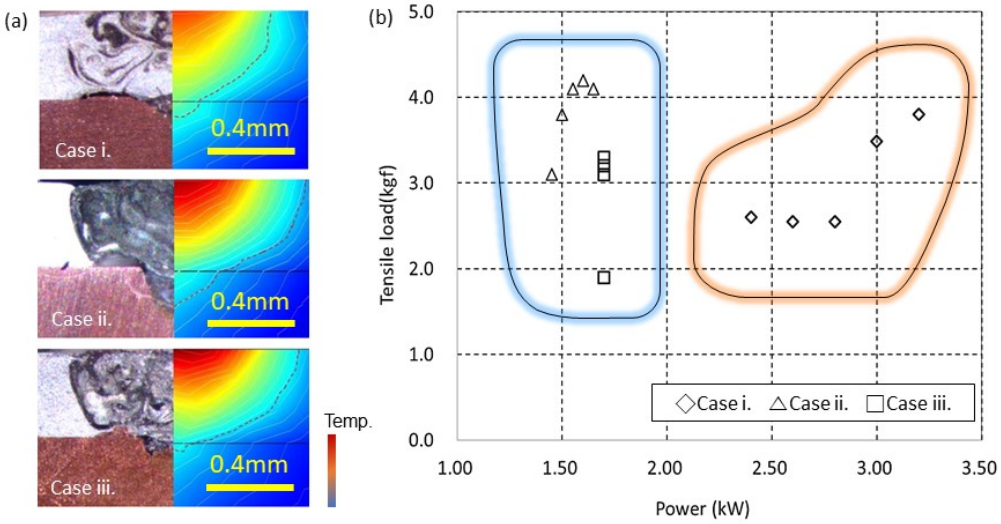

Figure 5. (**a**) Simulated thermal distribution (**b**) Summary of tensile load vs. heat input for each case.

All of the simulated factors of previous studies were 1; our figures are more similar to the experimental results. As an earlier study revealed that the optimal copper-layer penetration depth was 0.15 mm, we simulated depths of 0.05, 0.1, 0.15, and 0.2 mm; the respective temperatures were 1575.6, 857.3, 602.2, and 462.8 °C. The 0.15 mm value is closest to the experimental result.

To study the quenching effect, we simulated cooling rates after welding and compared them to the experimental results. The maximum temperature for a center beam of 800 W was 336 °C. On cooling, the temperature fell to 59 °C after 0.05 s. The temperature decrease was 82%, thus rapid. For the dual (center- and ring-) beam laser with a central beam of 800 W and a ring beam of 700 W, the maximum temperature was 518 °C. After 0.05 s of cooling, the temperature was 158 °C. The temperature reduction was 69%. Dual-beam laser welding thus afforded better cooling control than single-beam welding.

3.6. Effectiveness of Idea

Figure 5b combines results. The laser input powers ranged from 1.5 to 3.3 kW. At 2 kW, low and high heat input regions were discernible, and welding reliability was acceptable at 3 kgf. Excessive heat input did not necessarily increase weld strength. A comparison of Cases 1–3 revealed no proportional relationship between the welding strengths of the low and high heat input areas. Case 1 (◇) was associated with 2 to 3.3 kW input, but the welding strength was below 3 kgf. In Case 2 (△), the heat input was 1.5 to 1.7 kW, but

the welding strength remained excellent. In Case 3 (□), the laser beam wobbled, and the welding strength varied while the heat input remained constant.

In summary, joining dissimilar materials of aluminum and copper by laser welding presents specific challenges and requires a careful consideration of their disparate properties. Based on the results, there is a significant thermal mismatch, which reduces the joint's quality. Since aluminum has higher thermal conductivity and a lower melting point than copper, the thermal mismatch can result in uneven heat distribution during laser welding, leading to potential issues such as incomplete melting, excessive melt pool, or distortion. Aluminum and copper exhibit limited solubility in each other in their liquid state, which can form brittle intermetallic compounds at the weld interface. These intermetallic compounds can adversely affect mechanical properties of the joint such as strength and ductility.

Proper selection of laser parameters and joint design is crucial to mitigate the formation of intermetallic compounds and ensure a sound joint. In our experiment, the weld quality also depended on surface preparation. Due to the oxide layer of material that forms on aluminum surfaces and the potential for intermetallic compound formation at the weld interface, careful surface preparation is essential for successful dissimilar material joining of aluminum and copper by laser welding.

4. Conclusions

The experimental findings underscore the intricate interplay between laser beam modulation and the physical properties of dissimilar materials like aluminum and copper. The observed weld joint quality highlights the critical role of precise energy distribution. In Case 1, fixing the center beam output while varying the ring beam demonstrated how controlled pre- and post-heating can influence weld bead uniformity and tensile strength. However, excessive heat accumulation from the ring beam led to swelling in the upper weld zones, emphasizing the need for an optimal balance between the center and ring outputs. Case 2, on the other hand, showcased the advantages of modulating the core beam output, achieving superior tensile strength and bead uniformity compared to Case 1. These results suggest that a relatively low and stable ring beam output, combined with a modulated center beam, enhances energy efficiency while mitigating deformation risks. In Case 3, wobble welding further refined the control over heat distribution and weld quality. The smaller bead width and higher resolution of welds compared to Cases 1 and 2 signify the potential of wobble welding for applications requiring precision. The simulation results complement the experimental data by providing insights into the thermal dynamics of the weld pool, confirming that dual-beam laser setups achieve better cooling control and reduced thermal mismatches than single-beam systems.

Through this experimental study, we propose ring beam modulation-assisted laser welding on dissimilar materials. Note that the appropriate ring beam modulation enhances weld reliability. On cross-sectional analysis, finger-like penetrations were observed in the weld centers. Thus, energy consumption was effective, and reliable welding proceeded over minimal areas. When the core beam output was fixed, and that of the ring beam was varied, the weld beads were good, and the maximum allowable load increased as the output increased. However, as excessive heat from the ring beam traveled to areas affected by the center beam, the upper part of the weld became swollen, because the ring beam energy generated before and after welding diffused internally and became trapped, resulting in deformation. However, interfacial bonding occurred over a wide area, and the welding was nonetheless reliable. Swelling was not observed when the ring beam output was fixed at 500 W and that of the center beam varied. Therefore, to maximize the beneficial effects of pre- and post-heating, it is best to vary the output to the weld center and set the ring beam output relatively low.

Author Contributions: S.-H.C.: performed the experiments and analysis. J.-H.K.: draft the paper and figures by topics and editing. H.-W.C.: paper review, manuscript draft. All authors have read and agreed to the published version of the manuscript.

Funding: This research was funded by the Ministry of Trade, Industry and Energy of South Korea, grant no. RS-2024-00445669.

Institutional Review Board Statement: Not applicable.

Informed Consent Statement: Not applicable.

Data Availability Statement: Data sharing is not applicable to this article due to privacy.

Conflicts of Interest: The authors declare no conflicts of interest. The funders had no role in the design of the study; in the collection, analysis, or interpretation of data; in the writing of the manuscript; or in the decision to publish the results.

References

1. De Bono, P.; Blackburn, J. Laser welding of copper and aluminum battery interconnections. In Proceedings of the Industrial Laser Applications Symposium (ILAS 2015), Kenilworth, UK, 17–18 March 2015; Volume 96570. [CrossRef]
2. Kang, M.; Choi, W.S.; Kang, S. Ultrasonic and laser welding technologies on Al/Cu dissimilar materials for the lithium-ion battery cell or module manufacturing. *J. Weld. Join.* **2019**, *37*, 52–59. [CrossRef]
3. Das, A.; Li Williams, D.; Greenwood, D. Joining technologies for automotive battery systems manufacturing. *World Electr. Veh. J.* **2018**, *9*, 22. [CrossRef]
4. Abbaschian, L.; DFernandes Lima, M. Cracking susceptibility of aluminum alloys during laser welding. *Crack. Mater. Res.* **2003**, *6*, 273–278. [CrossRef]
5. Zheng, H.Y.; Huang, H. Ultrasonic vibration-assisted femtosecond laser machining of microholes. *J. Micromech. Microeng.* **2007**, *17*, N58. [CrossRef]
6. Stritt, P.C.; Hagenlocher, C.; Kizler, R.; Weber, R.C.; Ruttimann, C.; Graft, T. Laser spot welding of copper-aluminum joints using a pulsed dual wavelength laser at 532 and 1064 nm. *Phys. Procedia* **2014**, *56*, 759–767. [CrossRef]
7. Chopde, R.S. Study on laser beam welding of copper and aluminum joint. *J. Mech. Civ. Eng.* **2017**, *17*, 65–74. [CrossRef]
8. Zhou, X.; Zhang, G.; Shi, Y. Microstructures and mechanical behavior of aluminum-copper lap joints. *Mater. Sci. Eng. A* **2017**, *705*, 105–113. [CrossRef]
9. Kah, P.; Vimalraj, C.; Martikainen, J.; Suoranta, R. Factors influencing Al-Cu weld properties by intermetallic compound formation. *Int. J. Mech. Mater. Eng.* **2015**, *10*, 10. [CrossRef]
10. Cha, J.H.; Choi, H.W. Characterization of dissimilasr aluminum-copper material joining by controlled dual laser beam. *Int. J. Adv. Manuf. Technol.* **2022**, *119*, 1909–1920. [CrossRef]
11. Guo, S.; Zou, J.; Xu, J. Multi-stage keyhole evolution in fiber laser welding: An experimental study and theoretical analysis. *Results Phys.* **2021**, *31*, 104943. [CrossRef]
12. Cho, M.H.; Farson, D.; Lim, Y.C.; Choi, H.W. Hybrid laser/arc welding process for controlling bead profile. *Sci. Technol. Weld. Join.* **2007**, *12*, 677–688. [CrossRef]
13. Dijken, D.K.; Hoving, W.; Hosson, J.D. Laser penetration spike welding: A microlaser welding technique enabling novel product designs and constructions. *J. Laser Appl.* **2003**, *15*, 11–18. [CrossRef]
14. Stavridis, J.; Papacharalampopoulos, A.; Stavropoulos, P. Quality assessment in laser welding: A critical review. *Int. J. Adv. Manuf. Technol.* **2018**, *94*, 5–8. [CrossRef]
15. Lee, S.J.; Nakamura, H.; Kawahito, Y.; Katayama, S. Effect of welding speed on microstructural and mechanical properties of laser lap weld joints in dissimilar Al and Cu sheets. *Sci. Technol. Weld. Join.* **2014**, *19*, 111–118. [CrossRef]
16. Kim, T.; Choi, H.W. Study on Laser Welding of Al-Cu Dissimilar Material by Green Laser and Weld Quality Evaluation by Deep Learning. *J. Weld. Join.* **2021**, *39*, 67–73. [CrossRef]
17. Ning, N.; Zhang, N. Non-contact ultrasonic-assisted laser welding of copper hairpins. *J. Mater. Res. Technol.* **2024**, *31*, 3536–3550. [CrossRef]
18. Kim, Y.; Kim, C. Recent Trends about Modulation Technology of the Laser Beam Welding. *J. Weld. Join.* **2018**, *36*, 47–57. [CrossRef]
19. Kuryntsev, S. A Review: Laser Welding of Dissimilar Materials (Al/Fe, Al/Ti, Al/Cu)—Methods and techniques, microstructure and properties. *Materials* **2022**, *15*, 122. [CrossRef]
20. Lassila, A.; Andersson, T.; Ghasemi, T.; Lönn, D. Enhancement of joint quality for laser welded dissimilar material cell-to-busbar joints using meta model-based multi-objective optimization. *J. Adv. Join. Process.* **2024**, *10*, 100261. [CrossRef]

21. Cho, J.; Lee, T.; Bang, H.; Hyun, S.; Kim, C. Review on Laser welding technology on aluminum and copper dissimilar materials for secondary batteries assembly. *J. Weld. Join.* **2024**, *42*, 69–80. [CrossRef]
22. Han, C.M.; Kim, T.W.; Choi, H.W. Assessment of Laser joining quality by visual inspection, computer simulation, and deep learning. *Appl. Sci.* **2021**, *11*, 642. [CrossRef]
23. Lyu, H.; He, J.; Wang, C.; Jia, X.; Li, K.; Yan, D.; Lin, N.; Duan, J. Low-temperature sinterability of graphene-Cu nanoparticles:Molecular dynamics simulations and experimental verification. *Appl. Surf. Sci.* **2025**, *682*, 161683. [CrossRef]
24. Qi, J.; Liu, X. Femtosecond laser fabrication of infrared micro-optical devices based on hard and brittle materials and their applications. *Chin. J. Lasers* **2024**, *51*, 0402405.
25. Gattass, R.; Mazur, E. Femtosecond laser micromachining in transparent materials. *Nat. Photon* **2008**, *2*, 219–225. [CrossRef]
26. Neto, F.C.; Pereira, M.; Paes, L.S.; Fredel, C. Effect of power modulation frequency on porosity formation in laser welding of SAE 1020 steels. *Int. J. Adv. Manuf. Technol.* **2021**, *112*, 2509–2517. [CrossRef]
27. Chen, X.; Jiang, M.; Chen, Y.; Lei, Z.; Zhao, S.; Lin, S. Laser welding-brazing under temporal and spatial power modulation for dissimilar materials AA6061 to Ti6Al4V joints. *Manuf. Lett.* **2021**, *29*, 70–73. [CrossRef]
28. Liu, S.; Chew, Y.; Weng, F.; Sui, S.; Du, Z.; Man, Y.; Ng, F.; Bi, G. Effects of laser pulse modulation on intermetallic compounds formation for welding of Ti-6Al-4V and AA7075 using AA4047 filler. *Mater. Des.* **2022**, *213*, 110325. [CrossRef]
29. Jia, X.; Luo, J.; Li, K.; Wang, C.; Li, Z.; Wang, M.; Jiang, Z.; Veiko, V.; Duan, J. Ultrafast laser welding of transparent materials: From principles to applications. *Int. J. Extrem. Manuf.* 2025, *in press*. [CrossRef]